



e-ISSN: 2147-8228

www.dergipark.org.tr/ijamec

*Research Article***Epileptic seizure detection combining power spectral density and high-frequency oscillations****Rabia Tutuk ^{a,*} , Reyhan Zengin ^a** ^a*Department of Biomedical Engineering, Engineering Faculty, Inonu University, Malatya, Türkiye*

ARTICLE INFO

Article history:

Received 5 January 2023

Accepted 7 April 2023

Keywords:

Epilepsy

Maximum power

Ripples

Subband

ABSTRACT

Detection of pre-seizure signs in epileptic signals may help patients to survive the seizure with minimal damage. This study aims to detect epileptic seizure patterns using EEG datasets of five patients. The signals' maximum power spectral density (PSD) and high-frequency oscillations (HFOs) signals are investigated. The PSDs of all patients' signals are calculated, and the subbands of the maximum PSD are examined. It is observed that 95%, 85%, 85%, 75%, and 80% of the channels of the five patients are in the sum of delta and theta subbands of the maximum PSD, respectively. All patients' maximum power frequency subbands of F4 and T3 channels included only delta and theta subbands. Furthermore, frequency increase rates of pre-ictal and ictal signals are investigated, and increasing PSDs of ripples and fast ripples are then calculated. A much higher-frequency ripple follows the low-frequency ripple in 75%, 75%, 65%, 85%, and 75% of the channels of the first, second, third, fourth, and fifth patients, respectively. For the pre-ictal data, a much higher frequency ripple is not seen, followed by a low-frequency ripple in 90%, 85%, 75%, 90%, and 90% of all channels of five patients, respectively. In addition, in this study, the frequency of signals is observed to be 80 Hz and above in the Fp2, C4, P4, O2, and Pz channels, which are common to all patients. Consequently, examining PSD and HFO signals ensures the detection of the differences between the data sets and detects the epileptic seizure patterns in all five patients.

This is an open access article under the CC BY-SA 4.0 license.
(<https://creativecommons.org/licenses/by-sa/4.0/>)

1. Introduction

Epilepsy is a non-infectious chronic brain disease that influences nearly fifty million people of all ages globally. It consists of repetitive seizures resulting from aberrant electrical discharges in collective brain cells [1]. These can be caused by brain damage, head trauma, chromosomal and developmental disorders, hereditary diseases, and genetic or unknown reasons [2]. Epilepsy is a curable disease; however, despite all known treatments, seizures may not be controlled [3]. Due to these uncontrollable seizures, the quality of life of individuals with epilepsy decreases. Since the time and place of seizures are unknown, these people are in constant danger, so detecting seizures is crucial [9]. Due to this reason, in this study, the determination of the differences between healthy and epileptic seizure signals is investigated. In 1991, it was

shown in Spehlmann's EEG Primary book that EEG has great importance in the diagnosis of epilepsy and is effective in the differentiation of specific syndromes. The EEG was claimed to remain normal in 10% to 40% of epileptic cases. It explained that sleep, sleep deprivation, and hyperventilation (excessive breathing) facilitate the emergence of discharges in epileptic patients [4]. Meldrum and Chapman examined the synaptic release of amino acid neurotransmitters by in vivo microdialysis in 1999. They reported that extracellular hippocampal concentrations of glutamate and aspartate were increased before seizure onset in patients with epileptic foci in the temporal lobe [5]. Andrzejak et al. stated that there was a consistent decline in the strength of the delta subband in the pre-ictal term compared to the inter-ictal period [6]. Zhao et al. obtained a decrease in hemoglobin oxygenation 20 seconds before seizure onset [7]. It was also proposed that

* Corresponding author. E-mail address: rabiaturuk98@gmail.com
DOI: 10.18100/ijamec.1229907

ephemeral focal tissue oxygen deficiency and insufficient blood supply to the extremities are good signs for the epileptic centers and may occur before the outset of the ictal case [8]. Varvsky et al. stated that to fully agree with the epileptic brain, the period after the seizure is crucial regarding how the brain affects the seizure. They also defined structures like alterations in chemical (adenosine) or rebalancing of the chemical inequality accountable for on-setting the seizure [9]. As a result of a study conducted in 2012, individuals who have epilepsy were not nominees for surgical operation with vagal nerve stimulation for some patients; reducing or stopping the seizures was possible [10]. In 2014, the prediction of epileptic seizures was performed prospectively [11]. In the same year, Moghim and Corne noted that before the onset of seizures, an increase in the availability of oxygen, amount of oxygen in the blood, cerebral blood outflow, and any changes in heartbeat rate were involved [12]. Performing an analysis of venous blood gas based on pH, bicarbonate, base surplus, and lactate just one hour after the recent epileptic seizure attack could be used to predict the seizures [13]. In 2016, Teixeira et al. showed that before the onset of the seizure, a decrease in band power of the EEG since lower frequencies led to a decrease in the correlation process [14]. In addition, a method of predicting an epileptic seizure was proposed by combining a method of detecting changes in heart rate and identifying an abnormal condition [15]. Another study showed that impending seizures in multi-channel EEG data could be predicted with mean phase coherence, a measure of phase synchrony [16].

Lai and Chiang explained that automatic detection of epileptic seizures in EEG could be performed with machine learning methods using the dataset consisting of five different patient categories [17]. MJN Neuroserve developed a device that predicts epileptic seizures based on real-time stress and heart rate monitoring in 2018 [18]. After one year, Wang and colleagues automatically identified epileptic cases using a combination of Gradient Boosting Machine and system [19]. In another study, researchers developed an auto-detection method that effectively filters noise and considers the variability in EEG signals, potentially making it suitable for the clinical diagnosis of epileptic seizures [20]. Furthermore, an epileptic seizure detection focused on signal processing in the time-frequency domain with a multilevel Discrete Wavelet Transform (DWT) and nonlinear Artificial Neural Network (ANN) model was presented [21]. In 2020, Slimen et al. estimated that spikes in the ictal (during seizure) period increased compared to other periods, and spikes increased suddenly in the pre-ictal period compared to the inter-ictal period based on EEG sudden detection [22]. A recent study stated that continuous EEG monitoring is a standard approach for epilepsy detection to distinguish between epileptic seizures and non-epileptic seizures [23].

Power spectral density (PSD) is the most widely used feature for epileptic seizure detection. Spectral power properties such as absolute band powers in specific bands,

relative band powers, or spectral power ratios between these are known to be good properties for seizure detection or prediction [24].

Automatic analysis of the human EEG began in the early 1970s to help diagnose epilepsy. Total signal strength can be a useful measure of the difference in the variation between ictal and non-ictal EEG. In addition to variation in the aggregate signal power, it is feasible that the power in specific frequency bands would expose differences between epileptic and non-epileptic signals. The epileptic EEG generally includes spike and wave ingredients of frequencies up to approximately 20 Hz. It would be acceptable to await that the power of this frequency band, for a specific subject and recording, would be higher for epileptic EEG than non-epileptic one. A consistently higher mean power was demonstrated in the ictal EEG compared to the non-ictal period [25]. PSD has been used in many epileptic seizure classification studies to detect seizures in EEG segments. In similar studies, the PSD of each EEG data is calculated with different spectral analysis methods in addition to different feature extraction. These features are taken as input to classifiers, deep learning methods, or different machine learning methods. These methods have been used to optimize feature subsets such as PSD and to train the models [26, 27, 28, 29, 30, 31, 32, 33, 34]. In a study, spectral power was calculated in nine bands and used as a feature set for seizure prediction [35]. Another study in 2019 showed that the spectral power ratio in two distinct bands, rather than its characteristics in a particular band, can obtain better performance for seizure prediction, importantly [36]. Moreover, the spectral energy of the frequency subbands carrying the full information in the EEG signal was determined, and various subband combinations were obtained [37]. A recent study presented the feasibility of binary Hyperdimensional (HD) computation for detecting seizures from EEG data using local binary pattern (LBP) coding and PSD features. As a result of that study, it was seen that the PSD method outperformed the LBP method in test sensitivity, specificity, accuracy, and AUC (Area Under Curve) [38].

High-frequency oscillations (HFOs) are assigned as an influential factor in determining seizure activity. HFOs are promising biomarkers for epileptogenic tissue. HFOs are divided into ripples (R; 80–250 Hz) and fast ripples (FRs; 250–500 Hz). Most studies have reported higher HFO rates in epileptogenic tissue than non-epileptogenic tissue [39]. Recently, many studies have been done on the automatic detection of HFOs [40, 41, 42]. In 2021, Schoenberger et al. showed in an electrical stimulation study that 'pure' ripples, as opposed to epileptic surges, are essentially physiological [43].

This study used the well-known EEG dataset from the Department of Epileptology, University of Bonn,

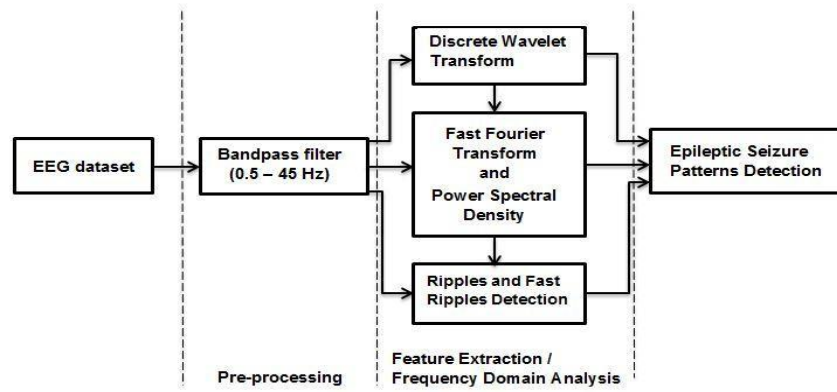


Figure 1. Steps of the epileptic pattern detection system

Germany. First, these datasets were preprocessed. Then, the EEG signals were divided into subbands, and the subbands with the maximum power spectral density were determined. These procedures were applied to healthy, pre-ictal, and ictal-containing datasets (A, C, E sets). In addition, the HFOs in the EEG signals and the maximum amplitude ratios of the pre-ictal and ictal EEG signals in the frequency subbands were calculated. The frequency values of the pre- and ictal EEG signals between the reference electrode (Fz) and the remaining channels were examined. Consequently, in this study, we determined the differences between healthy and epileptic seizure signals.

2. Materials and Methods

The flow diagram of the epileptic pattern detection system used in this study is given in Figure 1. First, EEG data is filtered with a band-pass filter as a preprocessing step. Secondly, due to the difficulties in the time domain, the signals are transformed into the frequency domain. Thirdly, the EEG signals are separated into subbands with the discrete wavelet transform (DWT) method to make the signals clearer. Then, the frequency subbands with the maximum PSDs of the signals are examined. After the HFOs in the signals are detected, the increasing value of the power spectral density (PSD) of ripples and fast ripples are calculated. Finally, with the resultant maximum PSD values and HFOs, epileptic seizure patterns can be detected.

2.1. Explanation of EEG data

The EEG dataset (well-known) used in this study was provided by the Department of Epileptology, University of Bonn, Germany, using a standard 10-20 electrode system (see Figure 2) [44]. The EEG dataset consists of 5 sets: A, B, C, D, and E. Each set contains 100 channels. A and B sets consist of EEG recordings from five healthy individuals. Set A consists of recordings taken with eyes open and set B with eyes closed. Other sets are taken from the EEG archive and belong to the pre-operative period. The signals in set D were recorded from the region that caused epilepsy. Set C was recorded from the opposite hippocampal part of the brain. C and D sets include only activity measured at non-seizure term.

Set E includes only seizure activities. The sampling frequency of the data is 173.61. All .txt files include 4096 samples [44]. EEG data of these five datasets were drawn with the MATLAB program (Figure 3). In this study, we decided to compare healthy (set A), pre-ictal (set C), and epileptic (set E) signals, so we used only A, C, and E datasets. We used sets A and E to classify healthy and epileptic data and set C to predict impending seizure activity.

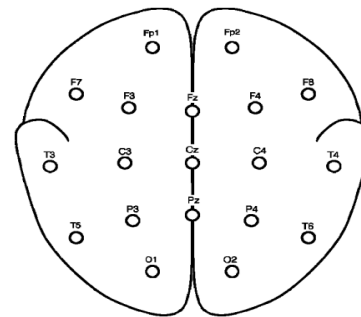


Figure 2. Positions of the surface electrodes correspondingly the international 10-20 electrode system [44]

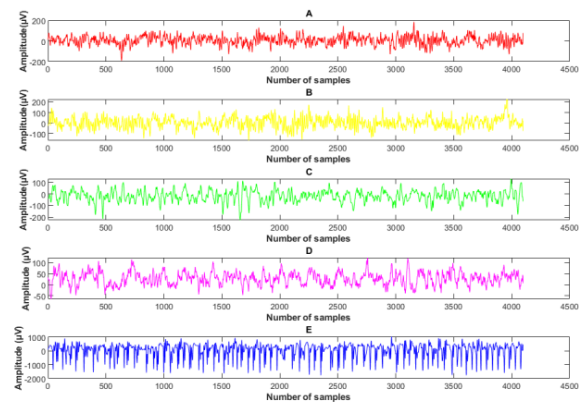


Figure 3. Graphical representation of EEG signals of A (healthy, eyes open), B (healthy, eyes closed), C (pre-ictal, opposite hippocampal), D (pre-ictal, epileptic region), and E (ictal) from first channel

2.2. Preprocessing of the EEG signals

One should do preprocessing to eliminate the noise in EEG signals. Many artifacts, such as eye-muscle movements or power line interference, may occur while recording EEG signals [45]. The frequency interval of EEG artifacts does not

usually exceed 50 Hz, device artifacts rarely exceed 30 to 40 Hz [46], and power line interference remains at 50 or 60 Hz [47]. Therefore, considering the EEG frequency bands, a band-pass filter is applied to limit the frequency of the signals between 0.5-45 Hz.

2.3. Discrete Wavelet Transform (DWT)

Discrete Wavelet Transform (DWT) is a method for decomposing non-stationary signals into different frequency subbands. However, it contains no physical comments about the signals [41]. This method splits signals into wavelet coefficients. Due to its conformity with variant-size windows, it ensures exact time and frequency knowledge at low and high frequencies. It enables the signal to be decomposed into coarse approximation and detailed knowledge with consecutive low and high pass filters. If the filter produces the coarse approximation and detail coefficients, it is called a low-pass and a high-pass filter, respectively. The sizes of coarse coefficients decrease by a factor of two in the subsequent decomposition. The time resolution is halved at each decomposition step, while the frequency resolution doubles (Figure 4) [45]. Choosing the most suitable separation level to perform the DWT process correctly is crucial. We can determine the number of decomposition levels according to the dominant frequency [45].

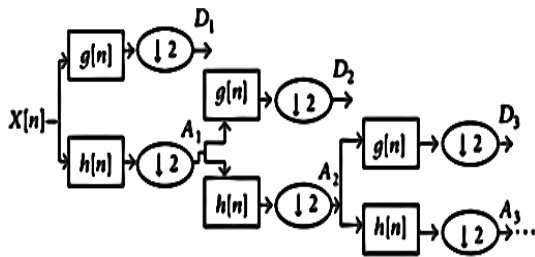


Figure 4. Application of discrete wavelet transforms [45]

2.4. Frequency Domain Analysis

In this study, we performed the frequency analysis of EEG signals. It is preferred due to its proven capability to distinguish between epileptic and non-epileptic EEG. Non-overlapping windows of EEG data with two seconds from a single channel are filtered in frequency bands to suit dual-style distributions in DWT analysis. These frequency bands are 2-4 Hz, 4-8 Hz, 8-16 Hz, and 16-32 Hz, which contain all frequencies of epileptic seizures and generally do not contain higher frequencies of artifacts. After filtering, each resultant frequency band's mean signal strength is computed [9].

2.5. Fast Fourier Transform (FFT) and Power Spectral Density (PSD)

EEG signals contain events with different frequencies. Most events are not always apparent in the time domain when cases at different frequencies interact [9]. PSD is an practical analysis method to determine EEG's static and dynamic properties. Dynamic features are reviewed to capture the time-varying nature of EEG. A locally stable behavior is

referred to as static property. The most common method used to detect epileptic seizures is PSD. The features of the EEG signals with PSD estimation are computed to symbolize these signals selectively. The PSD is computed with the Fourier transform of the autocorrelation sequence found by non-parametric methods [9].

Frequency transform is applied to the $y[n]$ signal to make our signal more understandable. With this transformation n [9] is defined as ω . Frequency transform can be used for any signal consisting of a linear combination of fundamental (basic) functions ($b_n[k]$, at time). These functions act as an implicit identity in the time domain and isolate the elements in time [9]:

$$b_n[k] = \begin{cases} 1 & \text{if } k = n \\ 0 & \text{otherwise} \end{cases} \quad (1)$$

The original signal ($y[n]$) in the time domain can be rewritten as follows:

$$y[n] = \sum_{k=-\infty}^{\infty} y[k]b_n[k], \quad n = 1, 2, 3 \dots \quad (2)$$

Fundamental functions in the frequency domain isolate the different frequency components of the $y[n]$ signal by projecting them into fundamental sinusoidal functions. These basic functions were chosen due to their excellent performance in isolating items with different frequencies. In the next step, the signal is defined in the frequency domain in the point of frequency components. Frequency domain analysis is known as a method for estimating frequency-related features.

For finite time domain signals with discrete time, the FFT of a random windowed signal $y[n]$ for $n = k + 1, k + 2 \dots, k + N$ is given by [9]:

$$FFT(\omega, k) = \sum_{n=1}^N y[n+k]e^{-i\omega n}, \quad \omega = \frac{2\pi m}{N} \quad (3)$$

The fundamental sinusoidal functions $e^{-i\omega n} = \cos(\omega n) - i \sin(\omega n)$ are able to isolate action at different frequencies ω , measured in terms of radians.

The FFT is defined for $0 \leq \omega = \frac{2\pi m}{N} < 2\pi$ with $m = 0, 1 \dots N - 1$. The range 0 to 2π is separated in equal divisions limited the number of samples in the windowed $y[n]$. To scale to correct the frequency sequence in Hz, a transformation of $\omega = 2\pi f/F_s$ is required, where F_s is the sampling rate of the data and f is the frequency in Hz among zero and F_s [9].

PSD is defined as a function of ω . It also contributes each frequency item to the strength of the resultant signal $y[n]$:

$$PSD[\omega, k] = |FFT[\omega, k]|^2 \quad (4)$$

where $|\cdot|$ specifies the absolute value. The concept of power is kept among the time and frequency domain [9]. In

this study, both PSD and maximum PSD were also investigated.

2.6. Ripples and fast ripples in the EEG signal

We aforementioned in Section 1 that oscillations in EEG signals are suitable biomarkers for seizure detection. They produce brain activities observed on EEG in the 80-500 Hz range, which are divided into high-frequency oscillations (HFOs) as ripples (80–250 Hz) and fast ripples (FRs; 250–500 Hz) [39]. HFOs are associated with seizures if there are HFOs in the transition from the pre-ictal to the ictal region. In addition, HFOs are increased from the inter-ictal (in the seizure-free period) to the pre-ictal periods and are spatially kept.

Ictal oscillations are mostly related to the seizure onset site. Just before the seizure, inhibitory and spike activities decrease. Then the epileptogenic activity of the tissue increases, and there is an increase also in HFOs. Therefore, in this study, a band-pass filter was first applied to the EEG signals using a sampling rate of 2 kHz to detect these ripples. As a result, signals with low-frequency components were eliminated, and signals with high-frequency (80-500 Hz) components were used [50]. The increasing PSD's of ripples and fast ripples were then calculated. Finally, the labeling process was carried out by normalization.

3. Results

In this study, we presented the methods for detecting the differences between healthy and epileptic seizure patterns. These methods were applied to all healthy and epileptic individuals, including the A, C, and E EEG data sets were taken from the Department of Epileptology, University of Bonn, Germany [44]. This study's calculations and signal processing steps were done online using Matlab (2021) [50]. First, the raw EEG signals were passed through a band-pass filter. Using the DWT method, the signals were decomposed into subbands, and the complexity of the signals was reduced [51]. Figures 5, 6, and 7 show the subband plots of sets A, C, and E with DWT, respectively.

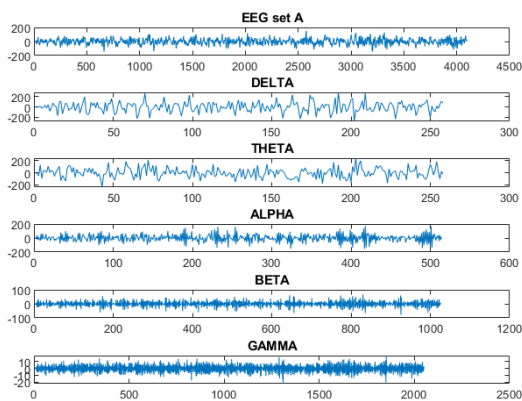


Figure 5. Discrete wavelet transform of EEG set A

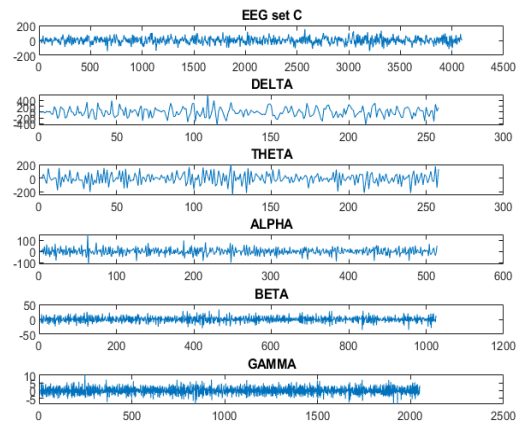


Figure 6. Discrete wavelet transform of EEG set C

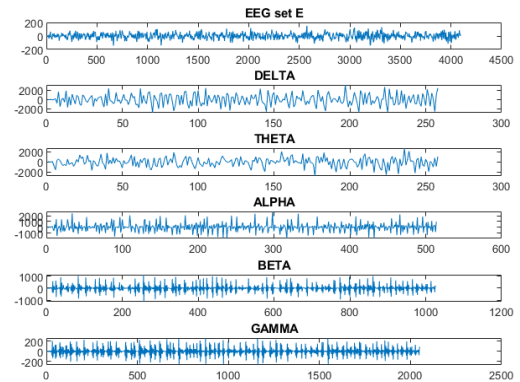


Figure 7. Discrete wavelet transform of EEG set E

Since EEG signals are not clear and comprehensible in the time domain, we applied Fast Fourier Transform (FFT). After FFT, we calculated the PSD of each signal and determined the frequency subbands with the maximum power. We compared each set with the PSD at each frequency subband. With this comparison, we determined the differences between healthy, pre-seizure, and epileptic EEG patterns.

In the frontocentral head regions, physiologically, the rhythm seen in deep sleep is the delta rhythm. In the case of generalized encephalopathy and focal cerebral dysfunction, the pathological delta rhythm occurs in awake states. People with temporal lobe epilepsy have temporal intermittent rhythmic delta activity (TIRDA). In the awake state, focal theta activity expresses focal cerebral dysfunction. The occipital head region in regular awake EEG recordings has a characteristic posterior dominant alpha rhythm. This rhythm is a feature of the normal background rhythm of adult EEG recording. It is known that in normal adults and children, the beta rhythm is the most common [49]. This pathological information of EEG subbands is the basis of our study.

Table 1. Frequency values and maximum PSD of each channels of five patients (Pat) in set E (* delta, * theta, * alpha, * beta, and * max (PSD)) Frequency value in maximum power (Hz) / Maximum PSD (V^2/Hz)($\times 10^4$)

	Pat-1	Pat-2	Pat-3	Pat-4	Pat-5	
Channels	Fp1	3.6/11.2	2.62/1.0	1.99/18.5	13.3/9.3	2.75/29.1
	Fp2	4.53/11.0	4.23/1.6	6.65/15.4	5.5/6.2	5.5/18.3
	F3	3.6/5.9	2.58/3.5	4.78/2.6	6.1/2.4	6.61/0.7
	F4	6.65/3.8	4.7/3.7	4.49/29.1	6.05/0.7	1.56/2.1
	C3	5.16/11.5	2.58/15.1	1.56/5.0	3.47/18.0	14.95/7.8
	C4	6.10/4.3	6.35/2.1	4.49/11.1	5.12/6.3	8.17/1.4
	P3	0.76/4.3	14.19/14.6	16.27/15.4	5.0/37.6	5.16/17.2
	P4	6.65/51.2	4.49/38.6	4.49/12.4	9.83/13.4	6.1/6.5
	O1	5.5/12.3	1.69/3.3	12.28/10.3	1.39/5.9	1.69/4.2
	O2	16.27/17.3	12.28/9.4	6.48/8.5	6.35/10.0	14.11/2.3
	F7	5.72/4.9	6.65/9.5	2.45/0.7	1.56/2.3	5.25/16.1
	F8	4.78/51.5	2.2/0.8	4.25/2.8	6.65/13.8	3.43/5.0
	T3	5.93/20.9	5.16/16.3	1.99/4.5	3.6/8.2	2.03/38.1
	T4	2.45/0.9	5.16/7.0	13.34/5.4	1.01/1.3	6.65/12.2
	T5	1.01/5.9	14.19/17.7	4.78/4.1	6.1/8.8	6.65/5.7
	T6	1.31/1.3	6.1/7.9	2.2/1.3	14.36/10.9	6.1/1.5
	Fz	4.53/23.3	1.94/15.6	6.65/10.4	11.77/0.6	6.65/48.0
	Cz	1.77/2.4	1.69/1.6	3.43/10.25	10.08/0.8	6.65/12.4
	Pz	3.6/18.3	5.65/1.9	4.49/51.7	5.29/25.8	9.57/9.8
	FCz	6.65/6.8	1.69/5.5	2.03/37.3	6.65/55.1	5.8/4.5

When the frequency subbands with maximum power are examined, in set E, maximum power is mainly seen in the delta and theta subbands. Also, a small part of the channels is in the alpha and beta subbands.

As given in Section 2.1, set E included only seizure activity. Since the E set includes delta and theta rhythms, our results are verified this information. Table 1 contains the maximum power calculated from the EEG signals of all channels of the five patients in the E set and the frequency

values with the maximum power.

Table 2 includes the percentages of the subbands of these frequencies (given in Table 1) in each channel according to the total channels. For example, examining Patient 1, one can see that 5% of the channels contain alpha and beta subbands, and 95% contain delta and theta subbands. Table 2 shows that these were epileptic signals for all patients in the E set. Apart from that, healthy, pre-seizure, and seizure signals were distinguished when the increase in PSDs of the A, C, and E sets was checked (not given in Table form).

Table 2. The percentage ratio of the number of frequencies in each subband of the set E to all frequencies in the total subband at maximum PSD (Pat: Patient)

	Alpha	Beta	Delta	Theta	Total (Alpha + Beta)	Total (Delta + Theta)
Pat-1	0.0	5.0	40.0	55.0	5.0	95.0
Pat-2	5.0	10.0	40.0	55.0	15.0	85.0
Pat-3	10.0	5.0	35.0	50.0	15.0	85.0
Pat-4	15.0	10.0	25.0	50.0	25.0	75.0
Pat-5	10.0	10.0	25.0	55.0	20.0	80.0

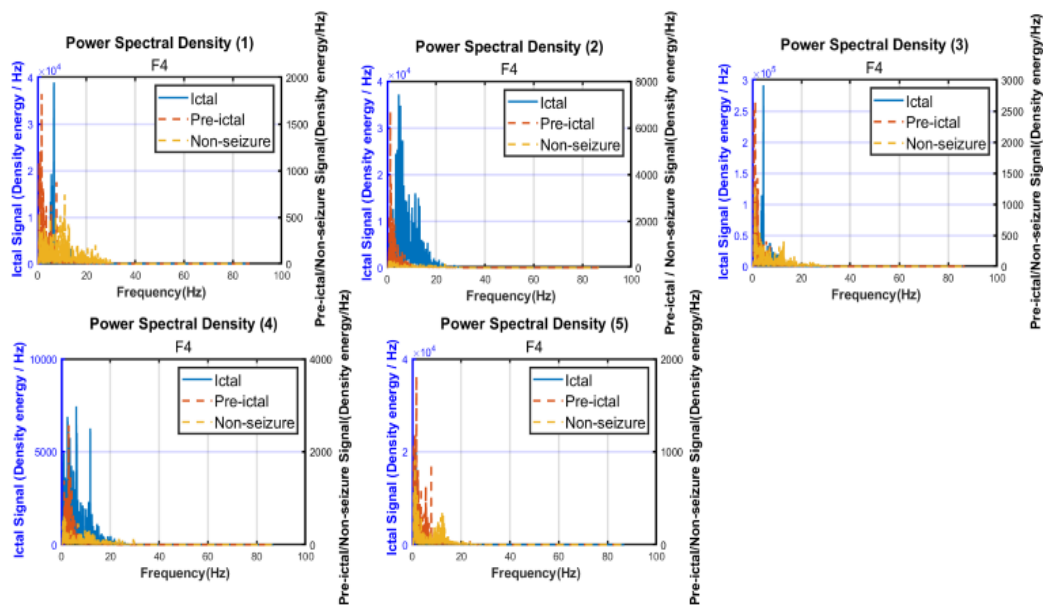


Figure 8. PSDs of the signals of the F4 channel of the all individuals (healthy and patient) of the sets A, C, E

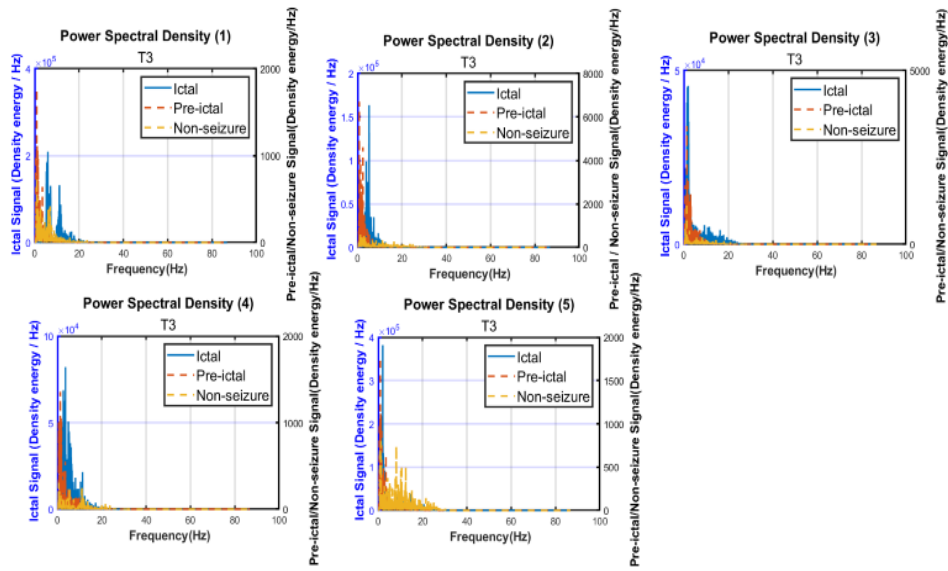


Figure 9. PSDs of the signals of the T3 channel of the all individuals (healthy and patient) of the sets A, C, E

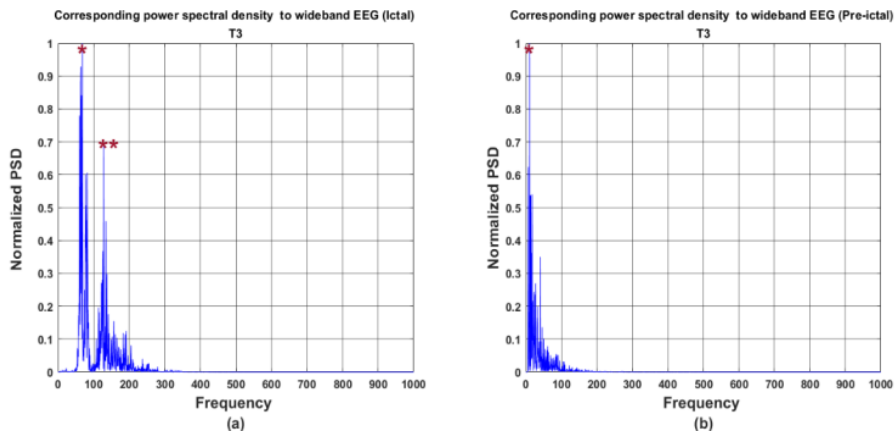


Figure 10. Corresponding power spectral density to wideband ictal and pre-ictal EEG signal (T3 channel)

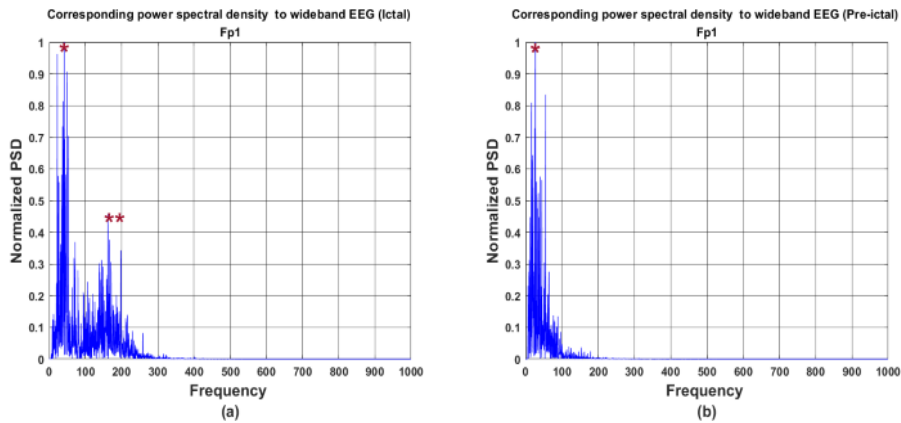


Figure 11. Corresponding power spectral density to wideband ictal and pre-ictal EEG signal (Fp1 channel)

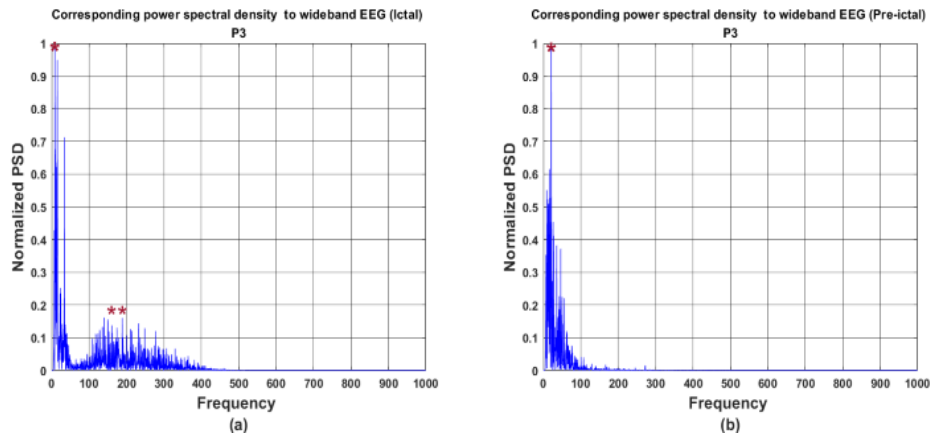


Figure 12. Corresponding power spectral density to wideband ictal and pre-ictal EEG signal (P3 channel)

We choose channels F4 and T3 due to the frequency subbands with maximum power, including only the delta and theta subbands for all patients. When the increases in PSDs of the A, C, and E sets were examined, it was seen that healthy, pre-seizure, and seizure signals were distinguished from each other. The PSDs of the F4 and T3 channels of the first and second individuals at these sets used in Figure 8 and Figure 9 are plotted, respectively. As can be seen from these figures, the PSD of the epileptic signal is higher than the PSD of the pre-seizure signal, and the PSD of the pre-seizure signal is higher than the PSD of the healthy signal. In particular, the PSD of the epileptic signal is considerably higher than the PSD of the healthy signal, which allows the two signals to be distinguished from each other. Furthermore, the healthy EEG signal frequency is spread over a wider band than the pre-seizure and epileptic EEG signals. Moreover, to distinguish the ictal and pre-ictal signals from each other, we used another method as HFOs in the EEG signals. When the EEG signals of each channel of each patient in the E dataset were examined, ripples and fast ripples were detected. A band-pass filter was first applied to the EEG signals using a sampling rate of 2 kHz to detect these ripples. As a result, signals with low-frequency components were eliminated, and just signals with high-frequency (80-500 Hz) components remained. The increasing PSD of ripples and fast ripples was then calculated. Finally, the labeling process was carried out by the normalization process.

We detected low-frequency ripples followed by many higher-frequency ripples in 75%, 75%, 65%, 85%, and 75% of the channels of the first, second, third, fourth, and fifth patients, respectively. Figures 10a, 10b, 11a, 11b, 12a, and 12b show the graphs obtained using broadband EEG segments representing HFOs in power spectral analysis using the criteria described in the methods (see Section 2.6). Figures 10a, 11a, and 12a shows how the HFO starts as a low-frequency swing (indicated as *) that turns into a much higher-frequency swing (indicated as **).

However, in Figures, 10b, 11b, and 12b, a much higher frequency ripple is not seen following the low-frequency ripple. This proves that Figures 10a, 11a, and 12a contain epileptic patterns. When the amplitude ratios between the pre-ictal and ictal signals are examined, the P3 channel was added because it is the common channel with an 80% amplitude increase. This channel was called the common channel because the 80% amplitude increase in all patients' preictal and ictal data was in the P3 channel. We chose the F4 and T3 channels as the maximum power for all epileptic data is only in the delta and theta subbands.

Table 3. Ripples (R) and fast ripples (FRs) in Fp2, C4, P4, O2, and Pz channels for all patients

	Fp2	C4	P4	O2	Pz
Pat-1	R	R	R	FRs	R
Pat-2	R	R	R	FRs	R
Pat-3	R	R	R	R	R
Pat-4	R	R	FRs	R	R
Pat-5	R	R	R	FRs	R

In five patients, frequency above 80 Hz was common in the Fp2, C4, P4, O2, and Pz channels. Table 3 shows the ripples and fast ripples found in these channels of five patients. In Fp2 and C4, ripples were present for all five patients, while in P4, ripples were detected for four patients and fast ripples for one patient. Ripples in the O2 channel were detected for two patients and fast ripples for three patients.

Ripples in the Pz channel were detected in five patients. Ripples and fast ripples were detected in other channels, but they are uncommon for all patients. The frequencies of the A and C data sets were generally found below 80 Hz. Thus, with this method, these data sets were distinguished.

In addition, we calculated the ratios of the frequency values between the reference electrode and all channels of these five patients' data to examine the frequency change between pre-ictal and ictal data.

Table 4. The ratios of the frequency values of the pre-ictal and ictal data between the reference electrode and all channels

		Pat-1	Pat-2	Pat-3	Pat-4	Pat-5
Ref-Ch	Fp1	138.8	195.45	-1100	62.4	153.7
	Fp2	109.8	81.6	109.1	81.4	200
	F3	109.7	309.5	123.07	600	116.6
	F4	100	140.8	119.3	328.5	181.05
	C3	88.57	176.19	372.2	77.3	95.4
	C4	7.6	132.7	62.06	91.6	100
	P3	115.5	112.5	101.4	161.5	80
	P4	-100	104.5	124.1	106.7	0
	O1	125.9	-100	109.1	100	104.3
	O2	100.8	113.2	109.5	0	99.5
	F7	100	93.1	100	109.1	75
	F8	84.1	250	40.3	100	107.8
	T3	64.7	150	-600	90.2	96.4
	T4	114.2	135.3	105.9	95.4	64
	T5	100.7	106.4	112.3	76.9	76
	T6	96.03	127.8	350	103.8	75
	Fz	102	733.3	85.3	87.6	-4
Cz	98.2	-100	145.4	100	-164	
Pz	116.6	129.05	77.5	190.6	95.7	

As mentioned in Section 2.6, HFOs increase during the transition from a seizure-free period to a seizure. As seen in Table 4, significant frequency changes are observed between the epileptic and pre-seizure signals. Thus, these frequency changes, usually observed as increases, indicate a pathological difference between the two signals. The negative values in Table 4 indicate a decrease in the frequency ratio, whereas the positive values indicate an increase in the frequency ratio. Thus, epileptic patterns can be detected with these rates, although not as much as other methods (PSD and HFO). The P3 channel, highlighted in this table, is the common channel with an 80% amplitude increase when the ratio between the pre-ictal and ictal signals is examined. As seen in Table 4, the frequency rates for five patients are 80% and above in this channel. This result can be used in channel selection studies.

4. Conclusion

This study deals with the methods for detecting epileptic seizure patterns. We determined the EEG signal subbands with maximum power for each signal in the A, C, and E data sets. It was determined by the maximum PSD method whether the detected subbands were pathological or non-pathological. The total percentage figures in Table 2 show that we correctly detected the ictal status for all five patients.

In addition, ripples and fast ripples were determined by frequency analysis of the signals. Frequencies in epileptic signals are generally found at 80 Hz and above. Furthermore, calculating the increased PSDs of ripples and fast ripples, it was observed that the HFO in epileptic data started as a low-

frequency ripple and then turned into a much higher-frequency ripple. However, pre-seizure data did not show much higher frequency ripples following the low-frequency ripples. Thus, the separation of epileptic patterns from pre-seizure patterns was also determined by this method. In ictal period, we detected low-frequency ripple followed by much higher frequency ripple in 75%, 75%, 65%, 85%, and 75% of all channels of the first, second, third, fourth, and fifth patients, respectively. For the pre-ictal data, we could not observe a much higher frequency ripple followed by a low-frequency ripple in 90%, 85%, 75%, 90%, and 90% of all channels of the first, second, third, fourth, and fifth patients, respectively. Table 4 shows big frequency changes between the pre-seizure and seizure periods in most channels for all five patients. This allows us to distinguish data containing epileptic patterns within five patients correctly.

In the future, these studies will be carried out to determine pre-ictal status with a larger data set. The aim is to create a communication system that automatically detects epileptic seizure signals for a certain period of time before the seizure occurs. Thus, epileptic patients can get through the seizure moment with the least damage by obtaining the pre-seizure differences of the brain signals.

References

- [1] World Health Organization, *Epilepsy*, pp. 1-2, 2022.
- [2] Sirven JI, "Epilepsy: A Spectrum Disorder," *Cold Spring Harb Perspect Med.*, 2015 Sep; 5(9): a022848. doi: 10.1101/cshperspect.a022848.
- [3] Akdağ et al., "Epilepsy," *Osmangazi Medical Journal*, 38 (Special Issue 1): 35-41, 2016. <https://doi.org/10.20515/otd.88853>.
- [4] Fisch BJ, *Spehlmann's EEG Primer*. Elsevier, pp. 634, 1991.
- [5] Meldrum BS, Chapman AG, "Excitatory amino acids receptors and antiepileptic drug development," *Jasper's Basic Mechanisms of the Epilepsies*, Delgado-Escueta, A. V. Wilson, W. Olsen, R. W. Porter, R. J. eds. Third Edition: Advances in Neurology, Vol. 79, 1999, Chapter 65:965-978 Lippincott Williams & Wilkins Philadelphia.
- [6] Andrzejak RG, Lehnertz K, Mormann F, Rieke C, David P, Elger CE, "Indications of nonlinear deterministic and finite-dimensional structures in time series of brain electrical activity: Dependence on recording region and brain state," *The American Physical Society*, volume 64, 061907, 2001. DOI: 10.1103/PhysRevE.64.061907.
- [7] Zhao M, Suh M, Ma H, Perry C, Geneslaw A ve Schwartz TH, "Focal Increases in Perfusion and Decreases in Hemoglobin Oxygenation Precede Seizure Onset in Spontaneous Human Epilepsy," *Epilepsia*, 48(11): 2059-2067, 2007. doi: 10.1111/j.1528-1167.2007.01229.x.
- [8] Schwartz TH, "Neurovascular Coupling and Epilepsy: Hemodynamic Markers for Localizing and Predicting Seizure Onset," *Epilepsy Curr.* 7(4): 91-94, Jul. 2007. doi: 10.1111/j.1535-7511.2007.00183.x.
- [9] Varsavsky A, Mareels I, Cook M, *Epileptic Seizures and the EEG/Measurement, Models, Detection and Prediction*. CRC Press, International Standard Book Number-13: 978-1-4398-1204-4 (eBook - PDF), 2011. <https://doi.org/10.1201/b10459>.
- [10] Bek S, Erdoğan E, Gökçil Z, "Vagal Nerve Stimulation and Patient Selection," *Epilepsy*, 18(Appendix 1): 63-67, 2012. DOI: 10.5505/epilepsi.2012.96168.
- [11] Meenakshi et al., "Frequency Analysis of Healthy Epileptic Seizure in EEG using Fast Fourier Transform," *International Journal of Engineering Research and General Science Volume 2*, Issue 4, June-July, 2014.
- [12] Moghim N, Corne DW, "Predicting Epileptic Seizures in Advance," *PLoS One*, 9(6): e99334, 2014. doi:

- 10.1371/journal.pone.0099334.
- [13] Kılıç TY, Yesilaras M, Atilla ÖD, Sever M, Aksay E, "Can venous blood gas analysis be used for predicting seizure recurrence in emergency department?" *World J Emerg Med*, Vol 5, No 3, 2014, doi: 10.5847/wjem.j.issn.1920-8642.2014.03.005.
- [14] Aguiar K, França FMG, Barbosa VC, Teixeira CS, "Early detection of epilepsy seizures based on a weightless neural network," *IEEE Engineering in Medicine and Biology Society (EMBC)*, Milan, 2016. DOI:10.1109/EMBC.2015.7319387.
- [15] Fujiwara K, Miyajima M, Yamakawa T, Abe E, Suzuki Y, Sawada Y, Kano M, Maehara T, Ohta K, Sakuma TS, Sasano T, Matsuura M, Matsushima E, "Epileptic Seizure Prediction Based on Multivariate Statistical Process Control of Heart Rate Variability Features," *IEEE TRANSACTIONS ON BIOMEDICAL ENGINEERING*, VOL. 63, NO. 6, JUNE 2016. doi: 10.1109/TBME.2015.2512276.
- [16] Aggarwal G, Gandhi TP, "Prediction of Epileptic Seizures based on Mean Phase Coherence," *bioRxiv preprint*, November 1, 2017. doi: <https://doi.org/10.1101/212563>.
- [17] Lai YF, Chiang GS, "Automatic Detection of Epileptic Seizures in EEG Using Machine Learning Methods," E-ISSN: 2224-2902, Volume 14, 2017.
- [18] Billeci L, Marino D, Insana L, Vatti G, Varanini M, "Patient-specific seizure prediction based on heart rate variability and recurrence quantification analysis," Sep 25; 13(9): e0204339, eCollection 2018, doi: 10.1371/journal.pone.0204339.
- [19] Wang et al., "Automated Recognition of Epileptic EEG States Using a Combination of Symlet Wavelet Processing, Gradient Boosting Machine, and Grid Search Optimizer," *Epilepsi*, 23(3): 109-117, 2017.
- [20] Hussein R, Palangi H, Ward RK, Wang ZJ, "Optimized deep neural network architecture for robust detection of epileptic seizures using EEG signals," *Clinical Neurophysiology 130*, 2019; 25-37, DOI: 10.1016/j.clinph.2018.10.010.
- [21] Abedin MZ, Akther S, Hossain MS, "An Artificial Neural Network Model for Epilepsy Seizure Detection," *5th International Conference on Advances in Electrical Engineering (ICAEE)*, 2019.
- [22] Slimen IB, Boubchir L, Seddik H, "Epileptic seizure prediction based on EEG spikes detection," *J Biomed Res.*, 2020 May; 34(3): 162-169, doi: 10.7555/JBR.34.20190097.
- [23] Stirling RE, Cook MJ, Grayden DB, Karoly PJ, "Seizure forecasting and cyclic control of seizures," 2020. <https://doi.org/10.1111/epi.16541>.
- [24] Zhang Z, Parhi KK, "Seizure detection using regression tree based feature selection and polynomial SVM classification," *37th Annual International Conference of the IEEE Engineering in Medicine and Biology Society (EMBC)*, 2015. DOI:10.1109/EMBC.2015.7319900.
- [25] McGrogan N, "Neural network detection of epileptic seizures in the electroencephalogram," *Oxford University*, 1999.
- [26] Srinivasan V, Eswaran C, Sriraam N, "Artificial Neural Network Based Epileptic Detection Using Time-Domain and Frequency-Domain Features," *Journal of Medical Systems*, Vol. 29, No. 6, December 2005. DOI: 10.1007/s10916-005-6133-1.
- [27] Tzallas AT, Tsipouras MG, Fotiadis DI, "Epileptic Seizure Detection in EEGs Using Time-Frequency Analysis," *IEEE Transactions on Information Technology in Biomedicine*, Volume: 13, Issue: 5, Sept. 2009. DOI: 10.1109/TITB.2009.2017939.
- [28] Ubeyli ED, "Statistics over features: EEG signals analysis," *Computers in Biology and Medicine*, pp. 733 - 741, 39 (2009). <https://doi.org/10.1016/j.compbiomed.2009.06.001>.
- [29] Bandarabadi M, Teixeira CA, Rasekhi J, Dourado A, "Epileptic seizure prediction using relative spectral power features," *Clinical Neurophysiology*, Volume 126, Issue 2, pp. 237-248, February 2015. <https://doi.org/10.1016/j.clinph.2014.05.022>.
- [30] Balasaraswathy N, Rajavel R, "Automatic seizure detection system with low complex PSD using TMS320C6713 DSP," *Int. J. Biomedical Engineering and Technology*, Vol. 18, No. 2, 2015. <https://doi.org/10.1504/IJBET.2015.070034>.
- [31] Ashokkumar SR, Anupallavi S, Premkumar M, Jeevanantham V, "Implementation of deep neural networks for classifying electroencephalogram signal using fractional S-transform for epileptic seizure detection," *Int J Imaging Syst Technol.*, 31: 895-908, 2021. <https://doi.org/10.1002/ima.22565>.
- [32] Nanthini K, Tamarasi A, Pyingkodi M, Kaviya SM, Mohideen PA, "Epileptic Seizure Detection and Prediction Using Deep Learning Technique", *2022 International Conference on Computer Communication and Informatics (ICCCI)*, Jan. 25 - 27, 2022. Coimbatore, INDIA.
- [33] Singh K, Malhotra J, "Smart neurocare approach for detection of epileptic seizures using deep learning based temporal analysis of EEG patterns," *Multimedia Tools and Applications*, 2022. <https://doi.org/10.1007/s11042-022-12512-z>.
- [34] Ma D, Zheng J, Peng L, "Performance Evaluation of Epileptic Seizure Prediction Using Time, Frequency, and Time-Frequency Domain Measures," *Processes*, 9(4), 682, 2021. <https://doi.org/10.3390/pr9040682>.
- [35] Park Y, Luo L, Parhi KK, Netoff T, "Seizure prediction with spectral power of EEG using cost-sensitive support vector machines," *Epilepsia*, Volume 52, Issue 10, pp. 1761-1770, October 2011. DOI: 10.1111/j.1528-1167.2011.03138.x.
- [36] Parhi KK, Zhang Z, "Discriminative Ratio of Spectral Power and Relative Power Features Derived via Frequency-Domain Model Ratio With Application to Seizure Prediction," *IEEE Transactions on Biomedical Circuits and Systems*, Volume: 13, Issue: 4, pp. 645 - 657, Aug. 2019. DOI: 10.1109/TBCAS.2019.2917184.
- [37] Tsipouras MG, "Spectral information of EEG signals with respect to epilepsy classification," *EURASIP Journal on Advances in Signal Processing volume 2019*, Article number: 10. 2019. <https://doi.org/10.1186/s13634-019-0606-8>.
- [38] Ge L, Parhi KK, "Applicability of Hyperdimensional Computing to Seizure Detection," *IEEE Open Journal of Circuits and Systems*, Volume: 3, pp. 59-71, 2022. DOI:10.1109/ojcas.2022.3163075.
- [39] Zweiphenning WJEM, Ellenrieder NV, Dubeau F, Martineau L, Minotti L, Hall JA, Chabardes S, Dudley R, Kahane P, Gotman J, Frauscher B, "Correcting for physiological ripples improves epileptic focus identification and outcome prediction," *Epilepsia*, 63: 483-496, 2022. <https://doi.org/10.1111/epi.17145>.
- [40] Kramer MA, Ostrowski LM, Song DY, Thorn EL, Stoyell SM, Parnes M, Chinappen D, Xiao G, Eden UT, Staley KJ, Stufflebeam SM, Chu CJ, "Scalp recorded spike ripples predict seizure risk in childhood epilepsy better than spikes," *Brain*, 142(5): 1296-1309, 2019 May 1. doi: 10.1093/brain/awz059.
- [41] Lachner-Piza D, Jacobs J, Bruder JC, Schulze-Bonhage A, Stieglitz T, Dümpelmann M, "Automatic detection of high-frequency-oscillations and their sub-groups co-occurring with inter-ictal-epileptic-spikes," *J Neural Eng*, 17(1): 016030, 2020 Jan 14;. doi: 10.1088/1741-2552/ab4560.
- [42] Nadalin JK, Eden UT, Han X, Richardson RM, Chu CJ, Kramer MA, "Application of a convolutional neural network for fully-automated detection of spike ripples in the scalp electroencephalogram," *J Neurosci Methods*, 360: 109239, 2021 Aug 1. doi: 10.1016/j.jneumeth.2021.109239.
- [43] Schönberger J, Knopf A, Dümpelmann M, Schulze-Bonhage A, Jacobs J, "Distinction of Physiologic and Epileptic Ripples: An Electrical Stimulation Study," *Brain Sci*. 11, 538, 2021. doi: 10.3390/brainsci11050538.
- [44] Andrzejak RG, Lehnertz K, Mormann F, Rieke C, David P, Elger CE, "Indications of nonlinear deterministic and finite-dimensional structures in time series of brain electrical activity: Dependence on recording region and brain state," *The American Physical Society, PHYSICAL REVIEW E, VOLUME 64, 061907*, 2001. DOI: 10.1103/PhysRevE.64.061907.
- [45] Bairagi RN, Maniruzzaman Md, Pervin S, Sarker A, "Epileptic seizure identification in EEG signals using DWT, ANN and sequential window algorithm," *Soft Computing Letters* 3, (2021) 100026.
- [46] Libenson M, "Practical approach to electroencephalography," First ed., *Saunders*, United States, 2009.
- [47] LeVan P, Urrestarazu E, Gotman J, "A system for automatic artifact removal in ictal scalp EEG based on independent component analysis and Bayesian classification," *Clinical Neurophysiology 117*, 912-927, 2006. <https://doi.org/10.1016/j.clinph.2005.12.013>.
- [48] Al-Fahoum AS, Al-Fraihat AA, "Methods of EEG Signal Features Extraction Using Linear Analysis in Frequency and Time-Frequency Domains", Volume 2014 |Article ID 730218, <http://dx.doi.org/10.1155/2014/730218>.
- [49] Nayak CS, Anilkumar AC, "EEG Normal Waveforms", Last

Update: July 31, 2021.

- [50] Park CJ, Hong SB, "High Frequency Oscillations in Epilepsy: Detection Methods and Considerations in Clinical Application," *J Epilepsy Res*, 9(1): pp. 1–13, 2019 Jun. doi: 10.14581/jer.19001.
- [51] Moctezuma LA, Molinas M, "EEG Channel-Selection Method for Epileptic-Seizure Classification Based on Multi-Objective Optimization," *Frontiers in Neuroscience*, Volume 14, Article 593, June 2020. <https://doi.org/10.3389/fnins.2020.00593>.
- [52] MathWorks Inc., "MATLAB [online]," Website <https://www.mathworks.com/products/matlab.html> [accessed 13 March 2022].
- [53] Bhavsar R, Helian N, Sun Y, Davey N, Steffert T, Mayor D, "Efficient Methods for Calculating Sample Entropy in Time Series Data Analysis," *Procedia Computer Science* 145, 97–104, 2018 . DOI:10.1016/j.procs.2018.11.016.
- [54] Zhong L, Wan J, Wu J, He S, Zhong X, Huang Z, Li Z, "Temporal and spatial dynamic propagation of electroencephalogram by combining power spectral and synchronization in childhood absence epilepsy", *Front. Neuroinform.*, 16 August 2022. <https://doi.org/10.3389/fninf.2022.962466>.